FEASIBILITY STUDY OF THE POTENTIAL USE OF CHEMISTRY BASED EMISSION PREDICTIONS FOR REAL-TIME CONTROL OF MODERN DIESEL ENGINES.

S. M. Aithal
Mathematics and Computer Science Division
Argonne National Laboratory
Argonne, IL 60439
aithal@mcs.anl.gov

D. Upadhyay
Scientific Research Laboratory
Ford Motor Company
Dearborn, MI, 48124
dupadhya@ford.com

ABSTRACT

The feasibility of using chemical kinetics-based prediction of emission species for real-time control of modern diesel engines is investigated. A previously developed fast, physics-based model is used as a representative example. The temporal variation of temperature required for the computation of the reaction rate constants is obtained from the solution of the energy equation. The effects of composition and temperature on the thermo-physical properties of the working fluid are included in the computations. Issues relating to model complexity, computation time, and fidelity are discussed in the context of both equilibrium and finite rate chemistry for use in the real time environment. The set of model inputs and tunable parameters is assessed for real-time use against the standard sensor set available on modern diesel engines. Results show that use of physics-based quasi-dimensional models is promising but may need complex variable mappings for real-time application.

NOMENCLATURE

E activation energy (J/mole)

h_{cg} convective heat transfer coefficient W m^{-2} K

H_P enthalpy of the products (J)

H_R enthalpy of the reactants (J)

i reaction index

I total number of reactions

k species index

$k_{f\,i}$ forward rate constant of the i^{th} reaction

k_{ri} backward rate constant of the i^{th} reaction

m instantaneous mass in the engine cylinder

$m_f(\theta)$ mass of fuel burned in crank angle θ (kg)

$n_k(t)$ number density of species k at time t

N_{rpm} rotational speed of the engine (rev/min)

P pressure (N/m^2)

P_1 pressure at BDC

R_g gas constant (J/kg-K)

R_u universal gas constant (J/K)

T(θ) average cylinder temperature at crank angle θ (K)

T_{adi} adiabatic temperature of the stoichiometric fuel-air

$T_r(\theta)$ temperature used to evaluate reaction rate constants at crank angle θ (K)

T_1 temperature at the beginning of the compression stroke (K)

V(θ) instantaneous volume at crank angle θ

Greek Symbols

β_I temperature exponent in the rate constant of the i^{th} reaction

γ ratio of specific heats

θ crank angle (degrees), CAD

υ_{ki} stoichiometric coefficient of the k^{th} species in the i^{th} reaction

υ'_{ki} stoichiometric coefficient of the k^{th} reactant species in the i^{th} reaction

υ''_{ki} stoichiometric coefficient of the k^{th} product species in the i^{th} reaction

1. INTRODUCTION

The modern diesel engine is a complex, dynamical system as such the real-time control (RTC) of diesel engines poses unique challenges. If we consider the four critical subsystems—injection, gas exchange, combustion, and emissions (including after-treatment)—and analyze the control objectives, the complexity of the processes and their underlying interactions quickly becomes evident. If we additionally consider the on-board diagnostics (OBD) requirements, as mandated by the California Air Resources Board and Environmental Protection Agency [1, 2], the level of complexity for Real Time Operation (RTO) is compounded. Consider for example the After-Treatment (AT) system. A typical AT system will comprise a diesel oxidation catalyst, a de-NO_x catalyst and a diesel particulate filter (DPF). The active control of the de-NO_x catalyst requires information on the feed gas (FG) NO_x; similarly, the active regeneration control of the DPF requires some information on its soot loading status, which is influenced by the FG soot concentration. In this document FG refers to the state of the engine exhaust exiting the engine. The need for information on FG NO_x and soot is therefore obvious. While FG NO_x may be measured (at substantial cost) soot sensors are not yet robust enough for use in mass produced vehicles. DPF regenerations are typically managed based on some soot loading metric derived from the pressure drop across the DPF [3]. The need for model-based predictions is also critical for states that cannot be sensed or for which a robust sensor does not exist. Modeling needs for other operating states maybe assessed at three levels, cost of using a sensor, OBD of the sensor (sensors are subject to OBD measures as well [1]), and failure mode actions in the event of a sensor failure.

Real-time models must be the best compromise between prediction fidelity and computational leanness. On the one end of the spectrum of fast RT usable models are empirical models that attempt to capture the essential sensitivities. These models are typically calibration intensive and may need to be retuned if the base engine calibration is altered. Alternatively, a reduced-order model may be extracted from a more elaborate physics-based model and cast as an implementable empirical model such as in [4]. Another approach would be to use zero-dimensional (also called quasi-dimensional) models as in [5 and references therein]. These quasi-dimensional models can be made more realistic and accurate by the inclusion of more physics describing the state of the working fluid during the compression and expansion stroke. For instance, the effects of mixture composition and temperature can be included in computing the thermophysical properties of the working fluid. Similarly, the fuel combustion can be described by an appropriate parameter so as to correctly predict the CA50 values for various operating conditions. Such a computationally efficient, physics-based model can be extended to include reduced reaction mechanisms for combustion and emission species formation. The temporal variation of temperature calculated by the solution of the energy equation can be used to compute the species concentrations with either finite-rate chemistry or equilibrium assumptions. In this work, we focus on the utility of such reduced order zero-dimensional models for RTO in the context of NO_x emission prediction for RTC.

2. REVIEW OF ENGINE MODEL TYPES, CAPABILITIES, AND LIMITATIONS IN THE CONTEXT OF RTC

Most models used in RTC are typically empirical as a result of operational constraints and often impose significant calibration burden. Using a fast physics-based approach can greatly aid in the development of robust and reliable models required for RTC. However, the development of such physics-based models is fraught with difficulties. This is largely due to the complex role that fluid-mechanics and combustion play in the formation of NO_x, soot and other unburned hydrocarbons in diesel engines. There is a close coupling of several physical and chemical processes such as droplet break-up, atomization, vaporization, and mixing followed by chemical reactions

that leads to the formation of various combustion products. Additionally, the formation of pollutants such as NO_x and soot are also strongly impacted by the operating conditions (RPM, load, fuel injection, EGR fraction, etc.), cylinder geometry, and mixture composition. Detailed numerical simulations coupling the fluid-dynamics and chemical reactions can provide an in-depth analysis of the spatial and temporal gradients of fluid-dynamics variables (temperature, pressure, gas velocities) along with species composition. However, these insights come at considerable computational cost. For example detailed mechanisms describing the pyrolysis of the fuel and the subsequent formation of NO require hundreds of reactions and species [6]. Inclusion of turbulence and mixing during the compression and expansion strokes also adds to the computational load. Typically, such simulations can take hours or days, depending on the available computational resources and complexity of the models. While these complex multidimensional models provide a great deal of insight into the mixing and combustion processes, the required computational time and resources preclude their use in real-time control. On the other hand, low-complexity, computationally fast, physics-based models (called quasi-dimensional models) can play a pivotal role in evaluating the impact of various operating conditions and engine parameters on performance and emission characteristics. Experimental data and detailed numerical simulations can play an important role in developing and validating such models. Typically, these quasi-dimensional models ignore spatial variation of fluid-dynamic variables and species concentrations. Temporal variation of an average cylinder pressure can be computed from the energy equation. Based on this temperature, an average engine temperature can be obtained [5]. The prediction of cylinder pressure and temperature can be made more accurate by computing mixture-averaged quantities of thermophysical properties such as enthalpy, internal energy, and ratio of specific heats. Combustion of the fuel and formation of pollutants is usually modeled using phenomenological considerations and reduced chemistry mechanisms.

3. ISSUES WITH QUASI-DIMENSIONAL MODELS

Since these low-dimensional models must mimic high-dimensional complex physical and chemical processes occurring during fuel injection and its subsequent combustion, they typically rely on a few tunable parameters, α_k. Ideally, these α_k not only must constitute the minimal set of parameters necessary for desired prediction fidelity but also must satisfy certain critical properties, namely,

$$\alpha_k = \varphi_k(x_i), \varphi_k \in C^m, x_i \in X_S, \tag{1}$$

for the model to be usable in RTC. Thus the "*k*" parameters, α_k, may be modeled as some function $\varphi_k(x_i)$ of the "*i*" nominally available variables, x_i, that belong to the set of nominally sensed or modeled variables X_S. A continuity constraint of order "m" maybe imposed on $\varphi_k(x_i)$ with, $m \geq 1$. Depending on the usage of α_k within the model structure, $m = 1$ guarantees smoothness of interpolation for transient operation over the operating space of the plant. The set of variables, X_S, includes all the directly sensed variables available from a standard sensor set as well as the set of inferred or modeled variables, such as exhaust gas flow rate that maybe inferred from the sensed variables, fresh air flow and injected fuel mass. Typically the α_k may be identified a priori and then used in the model. This may work well for scalar α_k; however, if α_k must be realized from a parameter space as a function of the operating conditions (as is often the case), then the impact of the projected α_k on the model prediction must be assessed in light of the overall prediction error.

4. MODEL PERFORMANCE NEEDS

4.1 Computation of species concentrations

Quasi-dimensional models used for RTC should be robust and fast. Solution of the energy equation (expressed in terms of the pressure and crank angle) provides the temperature and pressure required to compute species concentrations using either finite-rate chemical kinetics or equilibrium assumptions [5, 7]. Computations of the

species concentration can be time-consuming depending on the method of solution. For instance, Anderson et al. [7] computed temporal NO_x concentration based on equilibrium assumptions using a look-up table. This procedure can be time-consuming and cumbersome. A reduced chemistry NO_x model (6 reactions, 8 species) was used in [8] to compute the temporal NO_x concentration. Use of a robust implicit solver with variable time-stepping showed that finite-rate chemistry computations could be performed in about 60 milliseconds. Inclusion of reaction pathways to compute soot and CO would increase the computational time. Single-step or two-step phenomenological soot models can be used in conjunction with the mechanism described in [8] to obtain the temporal variation of both soot and NO_x. Impact of residual gas composition and initial conditions on the overall accuracy of the predicted NO_x have to be carefully examined. One approach worth exploring is the use of equilibrium chemistry computations in the duration between EOC and EVO to predict engine-out NO_x. Equilibrium concentrations depend only on the temperature, pressure and initial mixture composition. In a recent study, it was seen that equilibrium concentration of 20 species commonly encountered in combustion of hydrocarbon air mixtures could be obtained reliably in about 3–4 milliseconds [9]. The crank angle most appropriate for computing engine-out NO_x would have to be determined experimentally and would be one of the adjustable parameters in the quasi-one-dimensional model. Studies in [9] showed that the CO and concentration of soot precursors (such as C_2H_2 and C_nH_{n-1}) were not well predicted by equilibrium chemistry computations.

4.2 Sensor set assumptions

Whatever the modeling approach, it is critical that the modeling needs do not violate the standard sensor set assumptions, unless a clear and significant benefit can be demonstrated by adding additional sensors. While the cost constraint associated with sensors is obvious to most, what is typically ignored is the fact that all sensors that measure emissions must be monitored. Hence, adding sensors not only greatly increases the OBD burden but also makes the original equipment maker liable for warranty costs. Moreover, the possibility of a sensor failure cannot be ignored; hence all embedded codes for RTC must include a failure mode action associated with each sensor. It is

therefore obvious that models that do not comply with these requirements are best suited for offline analysis and cannot be used in RTC implementations. For completeness we discuss the standard sensor set found on most modern diesel engines and describe the variables that need sensing but must be predicted because of the inavailability of a robust sensor.

4.3 Gas exchange processes and combustion related parameters

Typically the gas exchange pathway is well instrumented. Information on fresh air and fuel flow rates and the essential manifold temperatures and pressures are available. In some applications the exhaust manifold pressure and temperature are predicted, and the exhaust gas flow rate often is inferred from air and fuel flows. The burnt gas fraction (BGF), or equivalently the oxygen content in the intake charge, is a critical parameter for diesel engines and is often inferred because of the lack of a reliable and robust EGR flow rate sensor. The intake oxygen may be sensed using an intake UEGO, which is a standard UEGO customized for use in the moist intake manifold environment. In Table 1we list the essential gas exchange parameters. The combustion-related parameters of interest and their associated needs are outlined in Table 2.

5. DESCRIPTION OF THE UNDERLYING MODEL

The numerical model used to study the compression and power stoke of a single-cylinder diesel engine is described in detail in [5]. Details of the model are presented here for completeness. Briefly, a zero-dimensional model was used to compute temporal variation of the temperature and pressure fields during the compression and power strokes. Temporal variation of the engine pressure and temperature during the compression and power stroke can be obtained by a numerical solution of the energy equation. Effects of temperature and mixture composition on the thermophysical properties of the working fluid were included in the solution of the energy equation. Temporal variation of the thermophysical properties of all the species in the gas mixture were obtained by using thermodynamic coefficients from the CHEMKIN database. Fuel combustion chemistry was modeled by a single-

step global reaction. The mass of fuel burned in each crank angle was determined using a fuel burn rate parameter so as to match the value of CA50 reported experimentally. The temporal evolution of NO_x was computed by using finite-rate chemical kinetics, coupled with a solution of the energy equation. NO_x formation was modeled by using a six step mechanism with eight species instead of the traditional equilibrium calculations based on the Zeldovich mechanism. The basic equations solved are given below.

$$\frac{dP(\theta)}{d\theta} = \frac{\gamma - 1}{V(\theta)}\left(Q_{in}(\theta) - Q_{loss}(\theta)\right) - \gamma \frac{P(\theta)}{V(\theta)}\frac{dV}{d\theta} \tag{2}$$

$$Q_{in}(\theta) = \left(H_P(T) - H_R(T)\right) \cong m_f(\theta) LHV \tag{3}$$

A fuel burn rate parameter was used to determine the number of fuel molecules burned during a given crank angle step and was used to compute Q_{in}. The fuel burn rate parameter is defined as the ratio between the molecules of hydrocarbons (N_p) at the end of a given crank-angle step to the number of molecules (N_r) at the start of the crank angle step. The difference between N_p and N_r equals the number of fuel molecules burned during a given crank angle step. The burn rate parameter was computed by using an exponential form.

$$br = e^{\frac{-A_b(\theta - \theta_{ig})}{(180 - \theta_{ig})}} = \frac{N_p}{N_r} \tag{4}$$

In Eq. (4) A_b is a constant, and θ_{ig} defines the start of ignition. Hence $br = 1$ implies no fuel burnt ($N_p = N_r$), and $br = 0$ implies complete combustion of the injected fuel. For this work θ_{ig} was established from the ignition delay $\theta_{id} = (\theta_{ig} - \theta_{soi})$, where θ_{soi} defines the crank angle of the start of injection. The ignition delay model used in this work was taken from [10] and is noted in Eq (5), the ignition delay varied in the range of 3 to 5 CAD after the start of injection.

$$\theta_{id} = (0.36 + 0.22Up) * \exp\left\{\begin{array}{l} E_A\_id\left[\left(\frac{1}{R_u T_1 CR^{\gamma-1}}\right) - \left(\frac{1}{17190}\right)\right]\cdots \\ \times\left[\left(\frac{21.2}{P_1 CR^{\gamma} - 12.4}\right)\right]^{0.63} \end{array}\right\} \tag{5}$$

The Q_{loss} in Eq. (2) is defined as follows.

$$Q_{loss}(\theta) = \frac{h_{cg} A}{\omega}(T(\theta) - T_w) \tag{6}$$

The value of the cylinder wall temperature, T_w, was set equal to the initial gas temperature at BDC ($T_w \sim 350$K). The instantaneous values of volume, area, and displacement, required for the solution of Eq. (2), are given by the slider-crank model and described in [5]. The convective heat transfer coefficient was expressed as

$$h_{cg} = 3.26 D^{-0.2} P^{0.8} T^{-0.55} w^{0.8} \tag{7}$$

where the velocity of the burned gas, w, is given by the following.

$$w = c_1 S_p + c_2 \frac{V_d T_r}{p_r V_r}(P(\theta) - P_m) \tag{8}$$

In Eq. (8), P_m is the motoring pressure. Specific heats, enthalpies, and internal energy of individual species in the working fluid were computed by using polynomials. Mixture-averaged values of the specific heat of the working fluid were averaged by using mole fractions as in [5, 8]. A similar procedure was used to compute the mixture-averaged values of enthalpy and internal energy of the working fluid. The average temperature of the gas in the cylinder can be obtained by

$$T(\theta) = \frac{P(\theta)V(\theta)}{m(\theta)R_g} \tag{9}$$

For each crank angle, the evolution of the concentration of species k is described by the rate equation

$$\frac{dn_k}{dt} = \omega_k \tag{10}$$

Here ω_k is the net production rate of species k due to all the I reactions considered in a given kinetics model, computed as shown below.

$$\omega_k = \sum_{i=1}^{I} (\upsilon_{ki} q_i), (k = 1, \ldots, K)$$
$$\upsilon_{ki} = \upsilon''_{ki} - \upsilon'_{ki} \tag{11}$$

$$q_i = k_{fi} \prod_{k=1}^{K} n_k^{\upsilon'_{ki}} - k_{ri} \prod_{k=1}^{K} n_k^{\upsilon''_{ki}} \tag{12}$$

$$k_{fi} = A_i T_r^{\beta i} \exp\left(\frac{-E_i}{RT_r}\right) \tag{13}$$

The reaction rate constants k_{fi} and k_{ri}, shown in Eq. (12), can be expressed in a form shown in Eq. (13). These rates are computed by using known constants and temperature obtained from the energy equation. As discussed in [8], the reaction rate constant in Eq. (13) is computed by using the average cylinder temperature for all crank angles except for $\theta_{ig} < \theta < \theta_{sc}$ during which period $T_r(\theta) = T_{adi}(\theta)$.

The model as discussed was exercised against steady-state data from [7]. For completeness we reproduce the model prediction from [8]. Model prediction was conducted for a validation data set comprising nine test points, as indicated in Table 3. Figure 1 shows the cylinder pressure evolution over the nine test cases concatenated to create a transient cycle. The cylinder pressure as shown is normalized against the cylinder pressure at BDC. In Fig. 2 we compare the predicted NO_x with the measured engine-out values. For information about the more extended model prediction capabilities with respect to EGR, air, and injection parameter variations, the reader is referred to the discussions in [8].

6. DISCUSSION ON THE MODEL IN THE CONTEXT OF RTC

We now present the rigorous exercise of assessing the proposed model for compatibility as an embeddable code for RTO. We begin with an examination of the tuning parameters and then assess the RT run time for the proposed model. The set of input parameters needed for this model is listed in Table 4, which shows that the input parameter set does not violate the criterion of availability as a standard variable. The tunable parameters used in this model are defined in Tab.5. The three critical parameters that can significantly influence the model prediction fidelity are A_b, θ_{SC}, and θ_{ig}. These parameters were identified a priori by optimization-based fitting. The convective heat transfer parameter, h_{cg}, is influenced by the two parameters c_1 and c_2, whose values are fixed by the Woschni model. The assessment of the model's RTC utility, from a calibration effort perspective, therefore essentially involves the

sensitivity of the modeled processes to the parameters, A_b, θ_{SC}, θ_{id}, or θ_{ig}. Note that since we know θ_{soi}, θ_{id} and θ_{ig} are dependent parameters, and hence identifying θ_{id} determines θ_{ig}.

The tunable parameters of interest are considered for compliance with RTO properties. The parameter θ_{SC} is the most critical parameter for this model since it is the only parameter fitted by using a cost function that minimizes a model prediction metric, FG NO_x in this case. Hence, once reasonable values for all other parameters have been achieved, the single parameter optimization of θ_{SC} implicitly considers any errors attributable to the parameters such as A_b, and θ_{id}. We will now assess properties of the tunable parameters for compliance for use in RTO against the data set in Table 3. We begin by assessing the parameter A_b, which is identified by matching the burn rate model against a measured heat release rate. In this work the CA50 value was used for identification. Figure 3 shows the A_b and θ_{SC} values identified for the nine cases as in Table 3. Clearly, these values cannot be interpreted as scalars, and therefore the underlying models (or surfaces) must be established for use in RTC such that the appropriate values for $A_b(k)$ and $\theta_{SC}(k)$ are available at each time step "k".

For illustration we show the impact of the base model prediction if the value of θ_{SC} is fixed to 3.5 CAD in Fig. 4. Large prediction errors were observed relative to the nominal prediction errors from the base model. In Test Case 9, for example, the prediction error increased from -35% to approximately -250%. The prediction error was defined as follows.

$$\varepsilon_{NO_x} = \frac{C_{NOx}^{mes} - C_{NOx}^{pred}}{C_{NOx}^{mes}} \tag{14}$$

It is clear that robust parameter update schemes must be identified and embedded in the real-time code.

In Fig 5 we show schematically the process for creating the A_b and θ_{SC} empirical models. It is also clear from the spread of the A_b and θ_{SC} parameters in Fig. 3 that the associated empirical models will be complex surfaces. In our initial exercise we used a Gaussian process model to identify θ_{SC}. The underlying θ_{SC} model that allowed the best base model predictions over the validation data set was indeed a complex surface without any immediate physical

significance associated to the mapping from the inputs to θ_{SC}. Similar checks with variations in parameters c_1 and c_2 did not yield any significant model prediction errors. This result was expected since the parameters c_1 and c_2 relate to a nominal process and the associated model as in Eqs. (7) and (8) is well established. The impact of, θ_{ig} and θ_{id} is realized through A_b.

7. PERFORMANCE OF A FULLY EMPIRICAL NO_X MODEL IMPLEMENTED IN RTC

A comparison of the kinetics-based model with a fully empirical and RT implemented model is necessary. Here we compare the predictions of the FG NO_x. The empirical model considered is based on the model in [4]. The implemented version of the model was extended to include several parametric sensitivities and deployed in several vehicles. The implementation burden included numerous 2-D surface and 1-D curves as well as several scalar parameters. This led to a substantial calibration effort where the prediction error was constrained be less than the requirements cascaded from OBD and AT control needs. This then necessitated the design of a full-scale automated calibration optimizer as well as an acceptable prediction error cost function for the calibration optimizer. As one would suspect, the prediction model was sensitive to base engine calibration changes.

Once tuned, however, the prediction was superior to both the steady-state and transient cycles, including off-cycle drives. Figure 6 shows a sample prediction of the model over a transient cycle. The prediction error, as in Eq. (14), never exceeded ±20%. The sensor valid flag indicates when the sensor output is valid. This compares well with the steady-state prediction error of the kinetics-based model that varied in the range +30% to -35%.

The fully empirical model associated with the predictions in Fig. 6 was implemented in RTC. The model was run at a 50 ms time step. Adding the model to the overall engine and aftertreatment control and diagnostics strategy on the processor computational burden did not have a significant impact. For the kinetics-based model, however, the impact of time marching of the species equations at each crank angle did turn out to be computationally expensive. In this work, an implicit time-marching scheme with variable time-stepping was used to reduce the computational burden. The total computational time for each operating condition in the transient depends on the number of crank-

angle steps during the compression and expansion stroke. The typical computational time for a compression and expansion stroke for simulations reported in [8] was about 60 milliseconds. From a standpoint of robustness of the implicit chemistry solver, the tuning parameters for the variable time-stepping must chosen to be stable for a range of operating parameters. Hence, the computational time per cycle of the transient can be around 100 milliseconds.

One could investigate the use of equilibrium chemistry computations as an alternative to finite-rate chemistry. The advantage of equilibrium chemistry is that the species composition depends on the temperature, pressure, and initial concentration of the cylinder charge. Therefore, one could compute the equilibrium NO_x concentration a few crank-angle degrees after the end of combustion and relate it to the engine-out NO_x. This approach requires the computation of equilibrium chemistry at a single point and could lead to substantial savings in computational time.

The chemistry-based modeling approach (finite-rate or equilibrium), however, has a clear advantage when it comes to calibration effort. Not only was the fully empirical model was very sensitive to the engine calibration level, but it also showed some engine-to-engine variability. The kinetics-based model, on the other hand, has the benefit of capturing most of the essential sensitivities through physics-based modeling. Hence the calibration effort reduces to creating response surfaces for two to three parameters only, as discussed. Additionally, these parameters can be expected to be relatively insensitive to engine calibration tweaks and engine-to-engine variations within a given engine model type.

8. CONCLUSIONS

The selection of the best modeling approach for RTC can be a challenging task. The essential trade-offs between the RT usage, calibration effort, commonality, and adaptability to different engine models are important considerations—but so are the considerations on prediction fidelity over steady-state and transient operations as imposed by control and diagnostic requirements. In this work we discussed in some detail a kinetics-based model in the context of RTC. We showed that it may be possible via order reduction to design physics-based models with a much reduced tunable parameter set. This approach promises a greatly reduced calibration burden. The

implementation burden on a RT processor was not assessed, but desktop runs showed promise. Currently we are assessing the performance of the proposed kinetics-based model under a fully transient cycle. This work will be followed by embedding the model in a processor for RTC.

ACKNOWLEDGMENT

This work was supported by the U.S. Dept. of Energy under Contract DE-AC02-06CH11357.

REFERENCES

[1] http://www.arb.ca.gov/homepage.htm.

[2] http://www.epa.gov.

[3] van Nieuwstadt M, Upadhyay D, Goeblebecker M, Ruona W. 2003. "Experiments in active diesel particulate filter regeneration," SAE 2003-01-3360.

[4] Upadhyay D, van Nieuwstadt M. 2003. "NOx prediction in diesel engines for aftertreatment control," ASME 2003-41196.

[5] Aithal SM. 2008. "Impact of EGR fraction on diesel engine performance considering heat loss and temperature-dependent properties of the working fluid," *Int. J. Energy Research* **33**,415-430.

[6] Miller JA, Bowman CT. 1989. "Mechanism and modeling of nitrogen chemistry in combustion," *Prog. Energy Combustion Sci*. **15(4)**, 287-338.

[7] Andersson M, Johansson B, Hultqvist A, Nöhre C. 2010. "A predictive real time NO_x model for conventional and partially premixed diesel combustion." SAE 2006-01-3329.

[8] Aithal SM. 2010. "Modeling of NOx formation in diesel engines using finite-rate chemical kinetics," *Applied Energy* **87(7),** 2256-2265.

[9] Aithal SM. 2011. “Equilibrium chemistry calculations for lean and rich hydrocarbon-air mixtures,” Argonne National Laboratory, Mathematics and Computer Science Division Preprint ANL/MCS-P1825-0111.

[10] Pulkrabek W. 2004. Engineering Fundamentals of the Internal Combustion Engine (2nd ed.). Prentice-Hall: Upper Saddle River, NJ.

List of Tables:

List of Figures

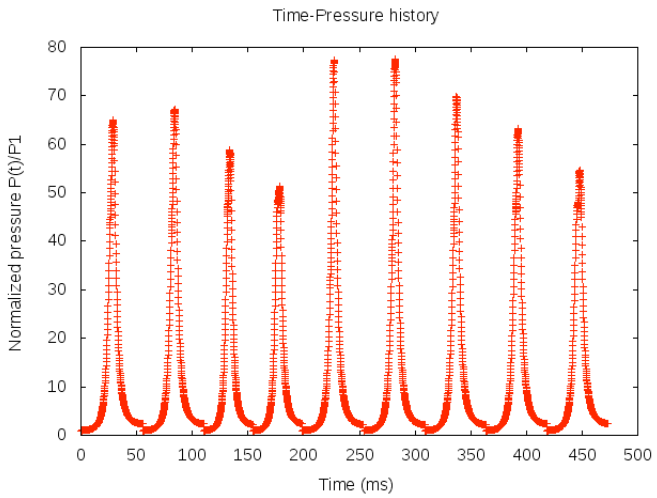

FIGURE 1. MODEL PREDICTION OF NORMALIZED CYLINDER PRESSURE

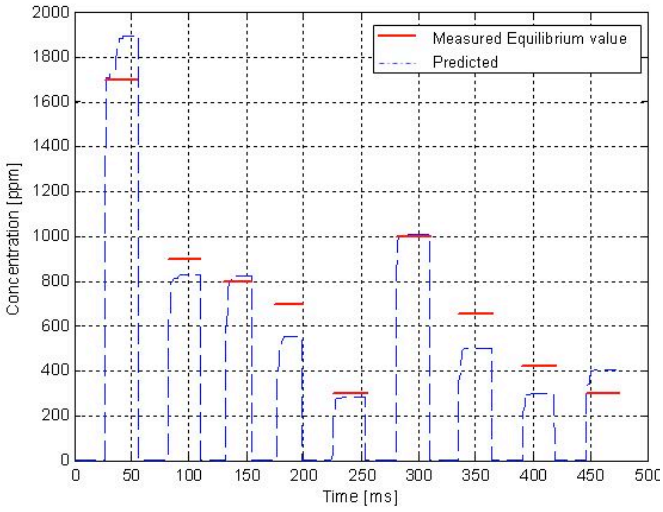

FIGURE 2. MODEL PREDICTION OF NO_x

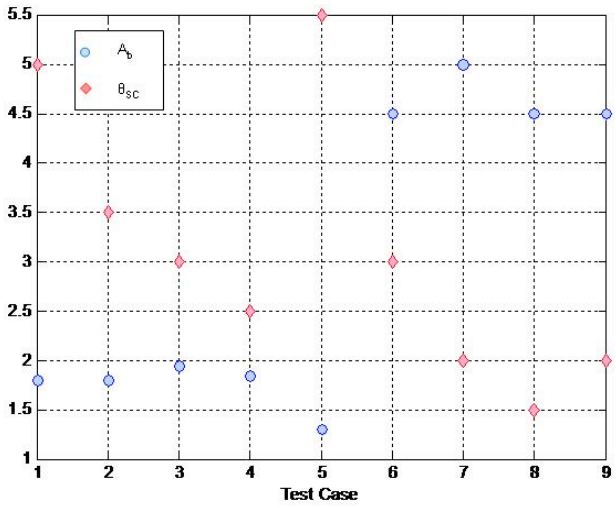

FIGURE 3. MODEL PARAMETERS A_b , θ_{SC}

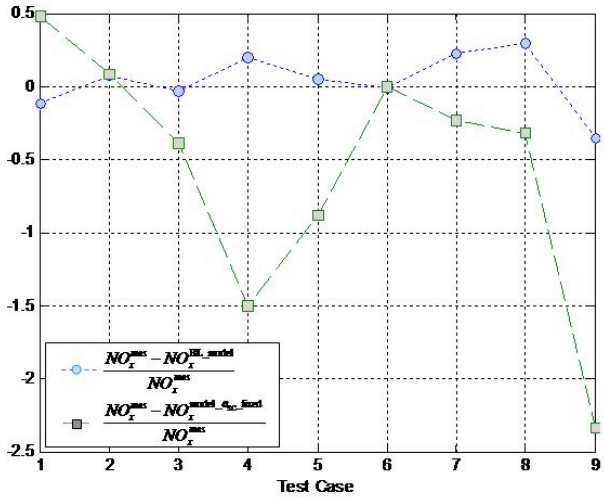

FIGURE 4. NO_x PREDICTION ERROR FOR θ_{SC} FIXED AT 3.5 CAD

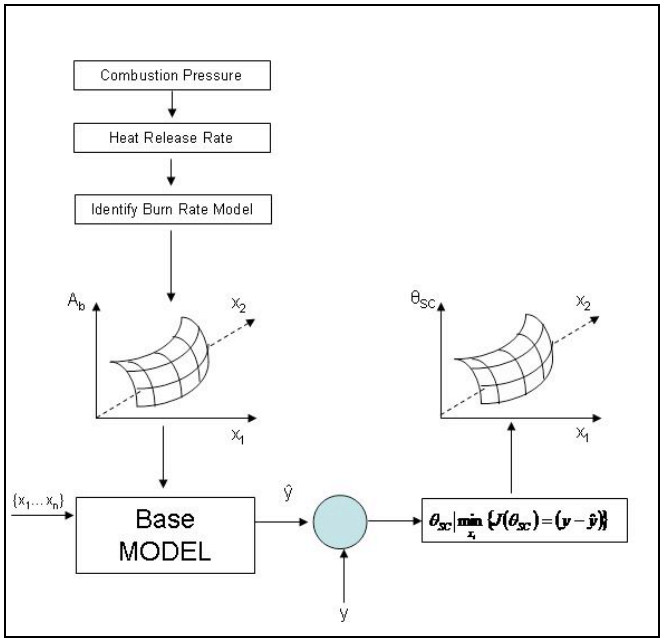

FIGURE 5. SCHEMATIC FOR PREDICTIVE MODELS FOR A_b AND θ_{SC} FOR USE IN RTC

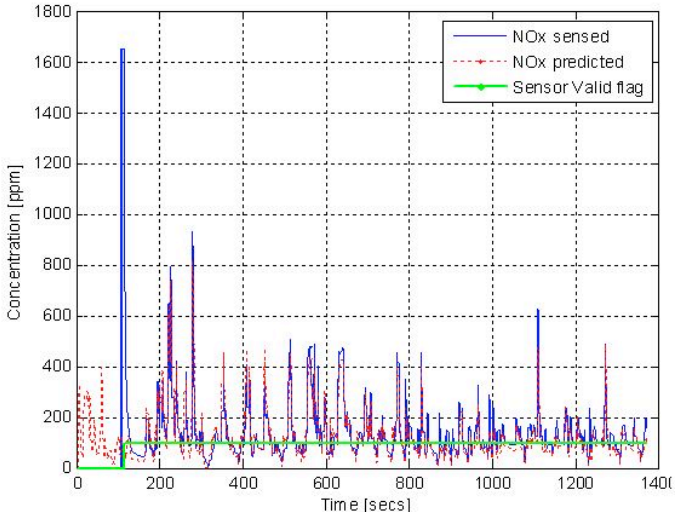

FIGURE 6. NO_X PREDICTION OF A FULLY EMPRIRICAL EMBEDDED MODEL FOR RTC

TABLE 1: ESSENTIAL GAS EXCHANGE PARAMETERS

Variable	Availability
Fresh air flow rate	Sensed
EGR flow	Modeled or sensed
Intake charge flow	Modeled
Intake charge temperature	Modeled
Intake O_2 or BGF	Currently predicted maybe sensed
Intake pressure	Sensed
Intake temperature	Sensed
EGR temperatures	Sensed or predicted
Turbo charger RPM	Mostly predicted, maybe sensed

TABLE 2: ESSENTIAL COMBUSTION-RELATED PARAMETERS

Variable	Availability
Fuel flow rate	Available
FG NO_x	Sensed or predicted
FG HC	Predicted if needed
FG CO	Predicted if needed
FG O_2	FG NO_x
Exhaust manifold temperature	Sensed or predicted
Exhaust manifold pressure	Sensed or predicted
Combustion pressure	Unavailable
Combustion temperature	Unavailable

TABLE 3: TESTCASE OPERATING CONDITIONS

N (rpm)	EGR (%)	Fuel (mg)	SOI (CAD)	P_1 (Bar)	Measured NO_x (ppm)
1090	4	120	171.5	2.5	1700
1090	23	65	171	2.5	900
1350	4	65	174	1.5	800
1350	3	72	178	1.5	700
1090	41	72	164	1.6	300
1090	26	66	167	1.5	1000
1090	26	66	171	1.4	650
1090	25	68	175	1.4	425
1090	25	68	179	1.4	300

TABLE 4: MODEL INPUTS

Variable	Availability
Cylinder geometry	Available
Engine speed	Available
Pressure at BDC	Intake pressure
Fresh air temperature	Sensed
EGR fraction	Predicted
EGR temperature	Sensed
Fuel injection rate	Available
Injection timing parameters	Available

TABLE 5: MODEL TUNABLE PARAMETERS

Parameter	Use
A_b	Model burn rate
θ_{SC}	Stoichiometric combustion duration
θ_{id}	Ignition delay
θ_{ig}	Start of ignition → θ_{id}